Dynamic Stability Control and Calculating Inverse Dynamics of a Single-link Flexible Manipulator

Nguyen Van Quyen [1], Bui Thi Hai Linh [2], Duong Quoc Tuan [3], Nguyen Trung Thanh [3], and Nguyen Hong Quang [3,*]

[1] Hanoi University of Science and Technology, Hanoi, Vietnam
[2] Faculty of Electrical Engineering, Thai Nguyen University of Technology, Thai Nguyen City, Vietnam
[3] Faculty of Mechanical, Electrical, Electronics Technology, Thai Nguyen University of Technology, Thai Nguyen City, Vietnam
* Coresspondence: quang.nguyenhong@tnut.edu.vn (N.H.Q.)

***Abstract*—When a robot manipulator operates at high speeds, the elastic vibration of its links is inevitable. To study this vibration phenomenon, the present paper deals with the problem of modelling, the dynamic stability control and calculating inverse dynamics of a single-link flexible manipulator. An algorithm to study dynamic stability and calculate inverse dynamics of flexible manipulators is proposed. The proposed algorithm is demonstrated and verified by the model of a flexible single-link manipulator. Through numerical simulation, the efficiency and usefulness of the proposed algorithm were demonstrated as well.**

***Keywords*—flexible manipulator, linearization, Taguchi method, dynamic stability, periodic system**

I. Introduction

Recently, flexible robots have been used in space technology, nuclear reactors, medical engineering, and many other fields. Flexibility, small volume, high speed, and low power consumption are advantages over rigid robots. However, the elastic displacements created by flexible links are the main cause of questions about position accuracy, structure stability and vibration. Some scientists have done research to solve those problems. However, the research results obtained are still relatively few and need to be studied further.

Recent valuable reviews on dynamics and control of flexible robots related to the existing works till 2016 are provided in some articles [1–4]. According to these works, the stability and vibration analysis of flexible robots have been little studied. It should be noted that in many applications of robot design and control, the computation of the full flexible model of a robot is not necessary, while the knowledge of its natural frequencies is required.

Bayo *et al*. [1] and Asada *et al.* [2] have proposed two different algorithms for calculating the torques required to move the end effector of flexible manipulators. A brief description of the development of stabile and vibration analysis of flexible manipulators has been depicted here. Some studies on the dynamic stability control of elastic manipulators have been presented in [3–13]. In general terms, an inverse dynamic problem for a serial manipulator is the problem of finding the joint torques that will produce a given end-effector motion. The inverse dynamics is originally designed to control the robotic manipulator. Motion control problems of flexible robots are divided into two classes: regulation and tracking control [14]. The regulation is the control problem around the desired equilibrium configuration of the robot. By the regulation $\mathbf{q}_d$ is constant, thus $\dot{\mathbf{q}}_d = \ddot{\mathbf{q}}_d = \mathbf{0}$. If the equilibrium configuration of the rigid robot is chosen as the fundamental motion, the equation for the error dynamics in first order approximation has the following form $\dot{\mathbf{x}} = \mathbf{A}\mathbf{x} + \mathbf{f}(t)$, where $\mathbf{A}$ is a constant matrix. The task of dynamic stability control is to determine the eigenvalues of matrix $\mathbf{A}$ of flexible manipulators [3–6]. Kumar and Pratiher [7] investigated the nonlinear phenomena of dynamic responses under 3:1 internal resonance in the two-link flexible manipulator. The tracking control in the joint space consists of a given time-varying trajectory $\mathbf{q}_d(t)$ and its successive derivatives $\dot{\mathbf{q}}_d(t)$ and $\ddot{\mathbf{q}}_d(t)$ which respectively describe the desired velocity and acceleration. In this case, $\mathbf{A}$ is no longer a constant matrix, but a time-varying matrix. Robots with flexible links are vibration systems. Therefore, the most important problem in robots with flexible links is the problem of determining the dynamic stability domain. Several schemes for performing these objectives do exist. Note that homogeneous linear differential equations or nonlinear autonomous differential equations can only be solved numerically. Therefore, the problem of dynamic stability control for the elastic manipulators in this case is usually only calculated by a numerical simulation method [8–13].

For the serial manipulator with rigid links, if the end-effector motion is known, inverse dynamics allows

Manuscript received August 6, 2022; revised October 13, 2022; accepted January 24, 2023.

doi: 10.18178/ijmerr.12.4.200-209

computation of the joint torques to the joints to obtain the desired motion of the end-effector. For the serial manipulator with flexible links, if the end-effector motion is known, we can not calculate the desired motion of the end-effector. Because we don't know the motion of the elastic coordinates. The inverse dynamics analysis for flexible robots by tracking control has been little studied, and the dynamic stability control of flexible manipulators is presently still an open problem. Robots with elastic links are vibration systems. Therefore, the most important problem in robots with flexible links is the problem of determining the dynamic stability domain. The main contribution of this paper is the study of dynamic stability control and the calculation of periodic vibration of a rigid-flexible link manipulator. Then it is possible to calculate the approximate force/torque of the actuators of the rigid-flexible link manipulator.

In this study, the linearization problem of the non-linear equations governing the motion of flexible manipulators in the vicinity of the periodic fundamental motion is addressed. A procedure based-Taguchi method [15–18] is proposed to design the control parameters of a controller PD for the system of a single-link flexible manipulator that is described by a linear differential system with time-periodic coefficients. Then the calculation of the actuator torques of the flexible manipulators is presented.

II. Dynamics of a Single-link Flexible Manipulator

A. Equations of Motion Using the Floating Frame of Reference Approach

Using the floating frame of reference approach [19], the motion equations for a single-link flexible manipulator shown in Fig. 1 are derived. As shown in the figure, a single-link flexible manipulator OE of length l with a rotor located at the hut and a payload at the free end. The end of the link is attached to the O point (including the motor) revolving around O-axis, and mass m_E is attached at E. The link is considered as a homogeneous beam with area A.

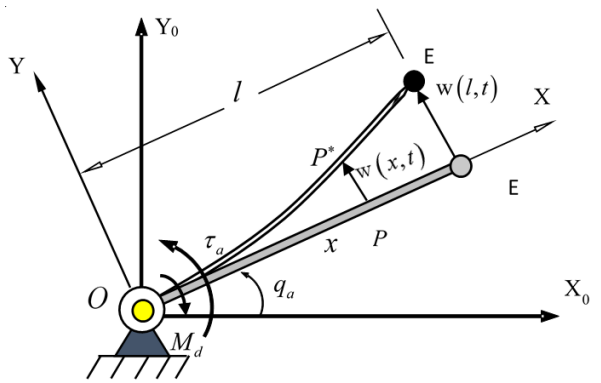

Figure 1. Single-link flexible manipulator.

To describe the kinematics, the position of point P on the flexible beam is given as:

$$\begin{aligned} x_P &= x\cos q_a - w(x,t)\sin q_a \\ y_P &= x\sin q_a + w(x,t)\cos q_a \end{aligned} \tag{1}$$

Differentiation of Eq. (1) yields

$$v_P^2 = \dot{x}_P^2 + \dot{y}_P^2 = (w^2 + x^2)(\dot{q}_a)^2 + \dot{w}^2 + 2x\dot{w}\dot{q}_a \tag{2}$$

It follows that

$$v_E^2 = (w_E^2 + l^2)(q_a)^2 + w_E{}^2 + 2lw_E q_a \tag{3}$$

The Euler-Bernoulli beam theory and Ritz-Galerkin method are applied to study the transverse vibration of the flexible link with assuming that the deformation in the longitudinal direction is negligibly small. Let the transverse deformation of the beam be written as:

$$w(x,t) = \sum_{i=1}^{N} X_i(x) q_{ei}(t),\ w_E = \sum_{i=1}^{N} X_i(l) q_{ei}(t) \tag{4}$$

where $q_{ei}(t)$ are unknown generalized coordinates of transverse deformation, $X_i(x)$ are a set of mode shapes of transverse deformation of a clamped-free beam and N is the number of modes used to describe the defection of the flexible link. The mode shapes are given as [20]:

$$\begin{aligned} X_i(x) &= \cos(\beta_i x) - \cosh(\beta_i x) \\ &+ \frac{\cos\beta_i l + \cosh\beta_i l}{\sin\beta_i l + \sinh\beta_i l}\left(-\sin(\beta_i x) + \sinh(\beta_i x)\right) \end{aligned} \tag{5}$$

The kinetic energy of the flexible manipulator is given by:

$$\begin{aligned} T &= T_1 + T_E + T_{OE} \\ &= \frac{1}{2} J_1 (\dot{q}_a)^2 + \frac{1}{2} m_E v_E^2 + \frac{1}{2}\int_0^l \rho A v_P^2 dx \end{aligned} \tag{6}$$

where J_1 is the mass moment of inertia of link 1 (including the motor) with respect to the point O, m_E is the mass at point E, ρA is the mass per unit length of the beam.

Substituting Eqs. (1), (2), (3) and (5) into Eq. (6), we obtain the kinetic energy of system

$$\begin{aligned} T &= (\frac{1}{2} J_1 + \frac{1}{2} m_E l^2 + \frac{1}{6}\rho A l^3)(\dot{q}_a)^2 \\ &+ \frac{1}{2} m_E [w_E^2 (\dot{q}_a)^2 + \dot{w}_E{}^2 + 2l\dot{w}_E \dot{q}_a] \\ &+ \frac{1}{2}\rho A \int_0^l \dot{w}^2 dx + \frac{1}{2}\rho A (\dot{q}_a)^2 \int_0^l w^2 dx \\ &+ \frac{1}{2}\rho A \dot{q}_a \int_0^l x\dot{w} dx \end{aligned} \tag{7}$$

The strain energy of the beam OE according to Reddy [21] is given by:

$$\Pi_e = \frac{1}{2} EI \int_0^l \left(\frac{\partial^2 w}{\partial x^2}\right)^2 dx \tag{8}$$

where E and I are the modulus of elasticity, area moment of inertia of the beam, respectively.

Substitution of Eqs. (1), (4) and (5) into Eq. (8) yields :

$$\begin{aligned}\Pi &= m_E g[l\sin q_a + \sum_{i=1}^{N} X_i(l)q_{ei}(t)\cos q_a] \\ &+ \frac{m_{OE} g l \sin q_a}{2} + \mu g \cos q_a \sum_{i=1}^{N} C_i q_{ei} \\ &+ \frac{1}{2} EI \sum_{i=1}^{N}\sum_{j=1}^{N} k_{ij}^{*} q_{ei} q_{ej}\end{aligned} \tag{9}$$

where

$$C_i = \int_0^l X_i dx \;;\; k_{ij}^{*} = \int_0^l X_i'' X_j'' dx \tag{10}$$

Lagrange's equations have the following form [22]:

$$\frac{d}{dt}\left(\frac{\partial T}{\partial \dot{q}_j}\right) - \frac{\partial T}{\partial q_j} = -\frac{\partial \Pi}{\partial q_j} + Q_j^{*},\ j = 1,2,\ldots,n \tag{11}$$

where q_j are the generalized coordinates which include rigid body coordinate q_a as well elastic modal q_{ei}, and Q_j^{*} are generalized forces. In this paper $Q_j^{*} = \tau_{aj} + M_{dj}$, in which M_{dj} is damping force which has the following form

$$M_d = \alpha \dot{q}_a \tag{12}$$

By substituting Eqs. (7), (9) and (12) into Eq. (11), we obtain the equations of motion of the system as:

$$\begin{aligned}&[J_1 + m_E l^2 + \frac{1}{3}\rho A l^3 + \rho A \sum_{i=1}^{N}\sum_{j=1}^{N} m_{ij} q_{ei} q_{ej} \\ &+ m_E \sum_{i=1}^{N}\sum_{j=1}^{N} X_i(l) X_j(l) q_{ei} q_{ej}]\ddot{q}_a \\ &+ [2m_E \sum_{i=1}^{N}\sum_{j=1}^{N} X_i(l) X_j(l) \\ &+ 2\rho A \sum_{i=1}^{N}\sum_{j=1}^{N} m_{ij}]\dot{q}_a \dot{q}_{ei} q_{ej} \\ &+ [\rho A \sum_{i=1}^{N} D_i + m_E l \sum_{i=1}^{N} X_i(l)]\ddot{q}_{ei} \\ &= -m_E g[l\cos q_a - \sum_{i=1}^{N} X_i(l) q_{ei} \sin q_a] \\ &- \frac{m_{OE} g l \cos q_a}{2} + \mu g \sin q_a \sum_{i=1}^{N} C_i q_{ei} + \tau - M_d\end{aligned} \tag{13}$$

$$\begin{aligned}&[m_E l X_i(l) + \rho A D_i]\ddot{q}_a \\ &+ [m_E X_i(l) \sum_{j=1}^{N} X_j(l) + \rho A \sum_{j=1}^{N} m_{ij}]\ddot{q}_{ej} + EI \sum_{j=1}^{N} k_{ij}^{*} q_{ej} \\ &- [m_E X_i(l) \sum_{j=1}^{N} X_j(l) q_{ej} + \rho A \sum_{j=1}^{N} m_{ij} q_{ej}]\dot{q}_a^2 \\ &= -m_E g X_i(l)\cos q_a - \mu g C_i \cos q_a\end{aligned} \tag{14}$$

$i = 1,2,\ldots,N.$

where

$$D_i = \int_0^l x X_i dx \;;\; m_{ij} = \int_0^l X_i X_j dx \tag{15}$$

If we choose $N = 1$ and use of symbols $q_{e1} = q_e$, the differential equations of the single-link flexible manipulator have the following form

$$\begin{aligned}&[J_1 + m_E l^2 + \frac{1}{3}\rho A l^3 + (\rho A m_{11} q_e^2 + m_E X_1^2(l) q_e^2)]\ddot{q}_a \\ &+ [\rho A D_1 + m_E l X_1(l)]\ddot{q}_e + [2m_E X_1^2(l) \\ &+ 2\rho A m_{11}]\dot{q}_a \dot{q}_e q_e + \frac{m_{OE} g l \cos q_a}{2} - \mu g \sin q_a C_1 q_e \\ &= -m_E g[l\cos q_a - X_1(l) q_e \sin q_a] + \tau - M_d\end{aligned} \tag{16}$$

$$\begin{aligned}&m_E X_1^2(l)\ddot{q}_e + m_E l X_1(l)\ddot{q}_a + \rho A D_1 \ddot{q}_a \\ &+ \rho A m_{11}\ddot{q}_e - m_E \dot{q}_a^2 X_1^2(l) q_e - \rho A \dot{q}_a^2 m_{11} q_e \\ &+ EI k_{11}^{*} q_e \\ &= -m_E g X_1(l)\cos q_a - \mu g \cos q_a C_1\end{aligned} \tag{17}$$

B. Linearization of the Motion Equations about the Fundamental Motion

We consider now the problem of linearizing motion equations of the single-link flexible manipulator in Fig. 1 as a demonstration example.

1) The fundamental motion

The fundamental motion of the considered manipulator is the virtual rigid link motion of link OE [2]. In this rigid-link motion, the position of the point *E* on the link is given as

$$x_E^R = l\cos q_a^R(t),\ \ y_E^R = l\sin q_a^R(t) \tag{18}$$

The mass moment of inertia of the virtual rigid link with respect to point O takes the form

$$J_O = \frac{1}{3}\rho A l^3 + m_E l^2 + J_1 \tag{19}$$

Using the momentum theorem, it follows that

$$\begin{aligned}\tau_a^R(t) &= M_d^R + (\frac{1}{3}\rho A l^3 + m_E l^2 + J_1)\ddot{q}_a^R(t) \\ &+ gl(\frac{1}{2}m_{OE} + m_E)\cos q_a^R(t)\end{aligned} \tag{20}$$

Assuming that the motion rule of the drive has the following form

$$q_a^R(t) = \frac{\pi}{2} + \frac{\pi}{2}\sin(\Omega t) \tag{21}$$

By differentiating Eq. (20) and then substituting the obtained result into Eq. (19) we have

$$\begin{aligned}\tau_a^R(t) &= \alpha \frac{\pi\Omega}{2}\cos(\Omega t) \\ &- \frac{\pi\Omega^2}{2}(\frac{1}{3}\rho A l^3 + m_E l^2 + J_1)\sin(\Omega t) \\ &+ gl(\frac{1}{2}m_{OE} + m_E)\cos(\frac{\pi}{2} + \frac{\pi}{2}\sin(\Omega t))\end{aligned} \tag{22}$$

From Eq. (20) the position of point *E* on the link is given as:

$$\begin{aligned}x_E^R &= l\cos q_a^R(t) = l\cos(\frac{\pi}{2} + \frac{\pi}{2}\sin(\Omega t)); \\ y_E^R &= l\sin q_a^R(t) = l\sin(\frac{\pi}{2} + \frac{\pi}{2}\sin(\Omega t))\end{aligned} \tag{23}$$

The fundamental motion of the manipulator is described by $\mathbf{q}^R(t)$ and $\boldsymbol{\tau}^R(t)$, where $\mathbf{q}^R(t)$ is the generalized coordinate of the manipulator

$$\mathbf{q}^R(t)=\begin{bmatrix} q_a^R(t) & q_e^R(t)\end{bmatrix}^T=\begin{bmatrix} q_a^R(t) & 0\end{bmatrix}^T \quad (24)$$

And $\boldsymbol{\tau}^R(t)$ is the torque

$$\boldsymbol{\tau}^R(t)=\begin{bmatrix} \tau_a^R & \tau_e^R\end{bmatrix}^T=\begin{bmatrix} \tau_a^R & 0\end{bmatrix}^T \quad (25)$$

In Eqs. (24) and (25) $q_e^R(t)$ denotes the elastic generalized coordinate and $\tau_e^R(t)$ the elastic torque of the virtual rigid link.

2) Linearization of the motion equations

The differential equations of the manipulator according to Eqs. (16) and (17) can be expressed in the following matrix form

$$\mathbf{M}(\mathbf{q})\ddot{\mathbf{q}}+\mathbf{C}(\mathbf{q},\dot{\mathbf{q}})\dot{\mathbf{q}}+\mathbf{g}(\mathbf{q})=\boldsymbol{\tau}(t) \quad (26)$$

where $\mathbf{q}$, $\dot{\mathbf{q}}$ and $\ddot{\mathbf{q}}$ are vectors of generalized coordinates, generalized velocity and acceleration, respectively

$$\mathbf{q}=\begin{bmatrix} q_a, q_e\end{bmatrix}^T, \boldsymbol{\tau}(t)=\begin{bmatrix} \tau_a(t), \tau_e(t)\end{bmatrix}^T=\begin{bmatrix} \tau_a(t), 0\end{bmatrix}^T \quad (27)$$

Let Δq_a and Δq_e are the difference between the real motion $\mathbf{q}(t)$ and the fundamental motion $\mathbf{q}^R(t)$, it follows that

$$q_a(t)=q_a^R(t)+\Delta q_a(t)=q_a^R(t)+y_1(t) \quad (28)$$

$$q_e(t)=q_e^R(t)+\Delta q_e(t)=y_2(t) \quad (29)$$

where y_1 and y_2 are called the additional motion or the perturbed motion. Similarly, we have

$$\boldsymbol{\tau}(t)=\begin{bmatrix} \tau_a(t), \tau_e(t)\end{bmatrix}^T=\begin{bmatrix} \tau_a(t), 0\end{bmatrix}^T \quad (30)$$

By substituting Eqs. (28), (29) into Eq. (24) and using Taylor series expansion around the fundamental motion, then neglecting nonlinear terms, we obtain a system of linear differential equations with time-varying coefficients for the manipulator as follows [22]

$$\mathbf{M}_L(t)\ddot{\mathbf{y}}+\mathbf{C}_L(t)\dot{\mathbf{y}}+\mathbf{K}_L(t)\mathbf{y}=\mathbf{h}_L(t) \quad (31)$$

Matrices $\mathbf{M}_L(t), \mathbf{C}_L(t), \mathbf{K}_L(t)$ and vector $\mathbf{h}_L(t)$ in Eq. (31) have the following forms

$$\mathbf{M}_L(t)=\begin{bmatrix} J_1+m_E l^2+\frac{1}{3}m_{OE}l^2 & \rho AD_1+m_E lX_1(l) \\ m_E lX_1+\rho AD_1 & m_E X_1^2(l)+\rho Am_{11}\end{bmatrix} \quad (32)$$

$$\mathbf{C}_L(t)=\begin{bmatrix} \alpha & 0 \\ 0 & 0\end{bmatrix} \quad (33)$$

$$\mathbf{K}_L(t)=\begin{bmatrix} k_{11} & k_{12} \\ k_{21} & k_{22}\end{bmatrix} \quad (34)$$

where

$$k_{11}=-l\sin q_a^R(t)m_E g-\frac{m_{OE}gl\sin q_a^R(t)}{2},$$
$$k_{12}=k_{21}=-m_E gX_1(l)\sin q_a^R(t)-\mu g\sin q_a^R(t)C_1,$$
$$k_{22}=-m_E[\dot{q}_a^R(t)]^2X_1^2(l)-\rho A[\dot{q}_a^R(t)]^2m_{11}+EIk_{11}^*.$$

And

$$\mathbf{h}_L(t)=\begin{bmatrix} 0 \\ -m_E gX_1(l)\cos q_a^R(t)-\mu g\cos q_a^R(t)C_1 \\ -m_E lX_1\ddot{q}_a^R(t)-\rho AD_1\ddot{q}_a^R(t)\end{bmatrix} \quad (35)$$

where fundamental motion $q_a^R(t)$ is given by Eq. (21) and constants $C_1, D_1, X_1, m_{11}, k_{11}^*$ are determined by Eqs. (5), (10) and (15). It should be noted that matrices $\mathbf{M}_L(t), \mathbf{C}_L(t), \mathbf{K}_L(t)$ and vector $\mathbf{h}_L(t)$ in this example are time-periodic with least period T. For numerical simulation, the calculating parameters of the considered manipulator are listed in Table I.

TABLE I. PARAMETERS OF THE MANIPULATOR

Parameters of the model	Variable and unit	Value
Length of link	$l(m)$	0.9
Sectional area of beam	A (m^2)	4×10^{-4}
Density of beam	ρ (kg/ m^3)	2710
Inertial moment of sectional area of beam	I (m^4) = $bh^3/12$	1.33333×10^{-8}
Modulus	E (N/m^2)	7.11×10^{10}
Mass moment of inertia of link 1 (including the motor)	$J_1(\text{kg.m}^2)$	5.86×10^{-5}
Mass of payload	m_E (kg)	0.1
Drag coefficient	$\alpha(N.m.s/rad)$	0.01

It follows from the parameters in Table I that

$$C_1=-0.7046317896,\ D_1=-0.4607100845,$$
$$m_{11}=0.8998501520,\ k_{11}^*=16.95515100,\ X_1=-2$$

III. Dynamic Stability Control of a Flexible Manipulator Using the Floquet Theory

In the steady of a flexible manipulator, the matrices $\mathbf{M}_L(t), \mathbf{C}_L(t), \mathbf{K}_L(t)$ and vector $\mathbf{h}_L(t)$ of the linear differential equations (31) are time-periodic with the least period $T=2\pi/\Omega$. For calculation of dynamic stability condition, we shall consider a system of homogeneous linear differential equations:

$$\mathbf{M}_L(t)\ddot{\mathbf{y}}+\mathbf{C}_L(t)\dot{\mathbf{y}}+\mathbf{K}_L(t)\mathbf{y}=0 \quad (36)$$

According to Floquet theory [25], the characteristic equation of Eq. (36) is independent of the chosen fundamental set of solutions. From characteristic equation of Eq. (36) we can calculate the Floquet multipliers $\rho_k(k=1,...,n)$. If $|\rho_k|<1$, the trivial solution $\mathbf{y}=0$ of Eq. (36) will be asymptotically stable. Conversely, the solution $\mathbf{y}=0$ of Eq. (36) becommes unstable if at least one Floquet multiplier has modulus being larger than 1. In this case we need to design the controller for stabilization the motion of flexible manipulator.

A. The PD Controller

It should be noted that the PD controller applied on the input link can be selected according to the formula:

$$\Delta\tau_a=-k_{d1}(\dot{q}_{\mathbf{a}}-\dot{q}_{\mathbf{a}}^R)-k_{p1}(q_{\mathbf{a}}-q_{\mathbf{a}}^R)=-k_{d1}\dot{y}_1-k_{p1}y_1 \quad (37)$$

The linearized equation according to Eq. (31) now takes the form

$$\mathbf{M}_L(t)\ddot{\mathbf{y}} + \mathbf{C}_L(t)\dot{\mathbf{y}} + \mathbf{K}_L(t)\mathbf{y} = \mathbf{h}_L(t) - \mathbf{K}_D\dot{\mathbf{y}} - \mathbf{K}_P\mathbf{y} \quad (38)$$

where $\mathbf{K}_D$ and $\mathbf{K}_P$ are diagonal matrices with positive elements as:

$$\mathbf{K}_D = \begin{bmatrix} k_{d_1} & 0 \\ 0 & 0 \end{bmatrix};\ \mathbf{K}_P = \begin{bmatrix} k_{P_1} & 0 \\ 0 & 0 \end{bmatrix} \quad (39)$$

It follows from Eqs. (38) that

$$\mathbf{M}_L(t)\ddot{\mathbf{y}} + [\mathbf{C}_L(t) + \mathbf{K}_D]\dot{\mathbf{y}} + [\mathbf{K}_L(t) + \mathbf{K}_P]\mathbf{y} = \mathbf{h}_L(t) \quad (40)$$

Eq. (40) can then be written in the form

$$\mathbf{M}_L^{(1)}(t)\ddot{\mathbf{y}} + \mathbf{C}_L^{(1)}(t)\dot{\mathbf{y}} + \mathbf{K}_L^{(1)}(t)\mathbf{y} = \mathbf{h}_L^{(1)}(t) \quad (41)$$

where

$$\mathbf{M}_L^{(1)}(t) = \mathbf{M}_L(t)\ ,\ \mathbf{K}_L^{(1)}(t) = \mathbf{K}_L(t) + \mathbf{K}_P\ ,$$
$$\mathbf{C}_L^{(1)}(t) = \mathbf{C}_L(t) + \mathbf{K}_D\ ,\ \mathbf{h}_L^{(1)}(t) = \mathbf{h}_L(t) \quad (42)$$

Eq. (41) can then be expressed in the compact form as:

$$\dot{\mathbf{x}} = \mathbf{P}(t)\mathbf{x} + \mathbf{f}(t) \quad (43)$$

where we use the state variable

$$\mathbf{x} = \left[\mathbf{y}^T, \dot{\mathbf{y}}^T\right]^T, \dot{\mathbf{x}} = \left[\dot{\mathbf{y}}^T, \ddot{\mathbf{y}}^T\right]^T \quad (44)$$

And the matrix of coefficients $\mathbf{P}(t)$, vector $\mathbf{f}(t)$ are defined by

$$\mathbf{P}(t) = \begin{bmatrix} \mathbf{0} & \mathbf{E} \\ -\mathbf{M}_L^{-1}\mathbf{K}_L^{(1)} & -\mathbf{M}_L^{-1}\mathbf{C}_L^{(1)} \end{bmatrix},\ \mathbf{f}(t) = \begin{bmatrix} \mathbf{0} \\ \mathbf{M}_L^{-1}\mathbf{h}_L^{(1)} \end{bmatrix} \quad (45)$$

To study the dynamic stability conditions of the manipulators, the properties of the homogeneous linear differential system corresponding to Eq. (43) is now considered:

$$\dot{\mathbf{x}} = \mathbf{P}(t)\mathbf{x} \quad (46)$$

where $\mathbf{P}(t)$ is a matrix of periodic elements with period T. Based on the stable criteria according to the Floquet multipliers [23], the gain values of the PD controller in Eq. (37) are chosen so that all Floquet multipliers of Eq. (46) have negative real parts and the transient oscillation time is as short as possible.

Based on these *Floquet multipliers* stability criteria of (46) are given as following:

- If the moduli of all the *Floquet multipliers* of the characteristic equation are less than the unity, then the periodic system Eq. (46) is asymptotically stable at the origin.
- If even one of *Floquet multipliers* of the characteristic equation has a modulus larger than unity, then the periodic system Eq. (46) is asymptotically unstable at the origin.
- If there is no *Floquet multiplier* of the characteristic equation with a modulus greater than unity, but there is a *Floquet multiplier* with a modulus equal to the unity, then the solution of the system of differential equations (46) may be stable, and may also be unstable, depends on the nonlinear terms.

B. A Procedure for Determination of Gain Values According to Floquet Multipliers Using the Taguchi Method

Taguchi method is a powerful technique to optimize performance of the products or process. Taguchi developed the orthogonal array method to study the systems in more convenient and rapid way, whose performance is affected by different factors when the system study become more complicated with an increase in the number of factors [14–17]. This method can be used to select the best results by optimization of parameters with a minimum number of test runs. We note that the Taguchi method has the following advantages: It is not necessary to use the derivative of the target function to calculate optimal parameters, and the method allows the determination of multiple stable parameters for the linear differential systems with time-periodic coefficients of complex structures.

Taguchi's approach to the product design process may be divided into three stages: system design, parameter design, and tolerance design. System design is the conceptual design stage where the system configuration is developed. Parameter design, sometimes called robust design, identifies factors that reduce the system sensitivity to noise, thereby enhancing the system's robustness. Tolerance design specifies the allowable deviations in the parameter values, loosening tolerances if possible and tightening tolerances if necessary.

Taguchi's objective functions for robust design arise from quality measures using quadratic loss functions. In the extension of this definition to design optimisation, Taguchi suggested the signal-to-noise ratio (SNR). Maximizing the SNR results in the minimization of the response variation and more robust system performance is obtained.

The most important task in Taguchi's robust design method is to test the effect of the variability in different experimental factors using statistical tools. The requirement to test multiple factors means that a full factorial experimental design that describes all possible conditions would result in a large number of experiments. Taguchi solved this difficulty by using orthogonal arrays (OA) to represent the range of possible experimental conditions. After conducting the experiments, the data from all experiments are evaluated using the analysis of variance (ANOVA) and the analysis of mean (ANOM) of the SNR, to determine the optimum levels of the design variables. The optimisation process consists of two steps; maximizing the SNR to minimize the sensitivity to the effects of noise, and adjusting the mean response to the target response.

In some cases, the optimal design is the least robust, and designers have to make a tradeoff between target performance and robustness. Ideally, one should optimise the expected performance over a range of variations and uncertainties in the noise factors.

Taguchi's techniques were based on direct experimentation. However, designers often use a computer to simulate the performance of a system instead of actual experiments.

We use the Taguchi method to determine the gain values of the PD controller. The target function is defined by the biggest modulus of Floquet multipliers and the target Floquet multiplier. The desired value of the target Floquet multiplier is usually chosen empirically.

In this section we present a procedure for determining the control parameters of the flexible manipulator shown in Fig. 1. This section presents an algorithm based on the Taguchi method to optimally design the gain values of the PD controller.

Step 1: Selection of control parameters and initial levels of control parameters

The gain values of the PD controller are chosen as components of the vector of control parameters which has the following form

$$\mathbf{x} = \begin{bmatrix} x_1 & x_2 \end{bmatrix}^T = \begin{bmatrix} k_{p1} & k_{d1} \end{bmatrix}^T \tag{47}$$

The initial three levels of each control parameter are chosen at random as shown in Table II.

TABLE II. CONTROL PARAMETERS AND INITIAL LEVELS OF EACH CONTROL PARAMETER

Levels	Control parameters	
	kp1	kd1
1	1	0.5
2	5	7
3	25	26

Step 2: Calculation of Floquet multipliers and selection of target function

The Floquet multipliers of Eq. (46) are calculated to the algorithms in [25] and can be arranged in a vector as follows:

$$\rho = [\rho_1 \quad \rho_2 \quad \rho_3 \quad \rho_4]^T \tag{48}$$

Step 3: Selection of orthogonal array and calculation of signal-to noise ratio (SNR)

Three levels of each control parameter are applied, necessitating the use of an L9 orthogonal array [16, 17]. Coding stage 1, stage 2, stage 3 of the control parameters are the symbols 1, 2, 3. The signal-to noise ratio (SNR) of control parameter **x** is evaluated using the following formula [16, 17]:

$$\eta_j = (\text{SNR})_j = -10\log_{10}(|\rho_{\max}|_j - \rho_d)^2, \quad j = 1,2,...,9 \tag{49}$$

where $|\rho_{\max}|_j$ is the biggest modulus of Floquet multipliers in the j^{th} experiment, and ρ_d is desired value of the target function. The desired value of the target function is usually chosen empirically. In this example we choose $\rho_d = 0.3$. The obtained results are shown in Table III.

TABLE III. DESIGN USING L9 ORTHOGONAL ARRAY

Trial (j)	Control parameters			Results
	kp1	kd1	$\lvert\rho\rvert_{\max}$	SNR
1	1	1	4.0561	−11.4948
2	1	2	1.2233	0.6930
3	1	3	1.0570	2.4184
4	2	1	0.4767	15.0542
5	2	2	0.6879	8.2258
6	2	3	0.9062	4.3473
7	3	1	0.4802	14.8872
8	3	2	0.0181	10.9991
9	3	3	0.4158	18.7229

Step 4: Analysis of signal-to-noise ratio (SNR)

Using the values of SNR of control parameters in Table III, we can calculate the mean value of the SNR of control parameters corresponding to the levels 1, 2, 3:

$\text{SNR}(k_{p1}^1)$=[SNR(1)+SNR(2)+SNR(3)]/3=-2.79447

$\text{SNR}(k_{p1}^2)$=[SNR(4)+SNR(5)+SNR(6)]/3=9.2091

$\text{SNR}(k_{p1}^3)$=[SNR(7)+SNR(8)+SNR(9)]/3=14.86973

$\text{SNR}(k_{d1}^1)$=[SNR(1)+SNR(4)+SNR(7)]/3=6.148867

$\text{SNR}(k_{d1}^2)$=[SNR(2)+SNR(5)+SNR(8)]/3=6.6393

$\text{SNR}(k_{d1}^3)$=[SNR(3)+SNR(6)+SNR(9)]/3=8.4962

In which

$$\text{SNR}(k_{p1}^1), \text{SNR}(k_{p1}^2), \text{SNR}(k_{p1}^3), \text{SNR}(k_{d1}^1), \text{SNR}(k_{d1}^2), \text{SNR}(k_{d1}^3)$$

are the mean square deviation of the control parameters $k_{p1}^1, k_{p1}^2, k_{p1}^3, k_{d1}^1, k_{d1}^2, k_{d1}^3$ at the levels 1, 2, 3, respectively. Then the SNR of the control parameters can be plotted to use for optimization of seat displacement as shown in Fig. 2.

From Fig. 2, the optimal signal-to-noise ratio of the control parameters can be derived as follows:

$$\text{SNR}\ (k_{p1}) = 14.86973, \text{SNR}\ (k_{d1}) = 8.4962 \tag{50}$$

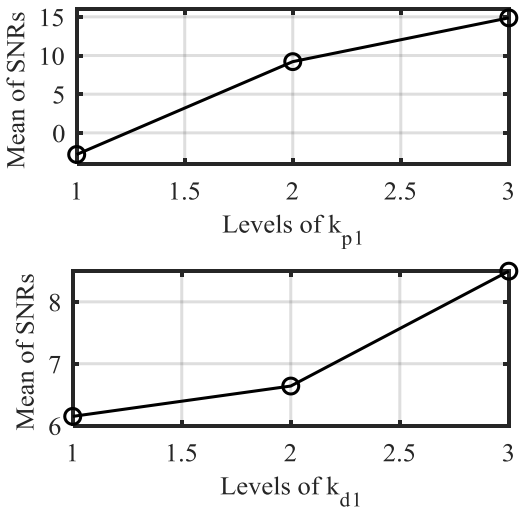

Figure 2. Diagram of level distribution of mean signal-to-noise ratio of the control parameters.

Step 5: Selection of new levels for control parameters

From Eq. (50), it can be seen that the optimal SNR of the control parameters is different. This makes it easy to perform iterative calculation. Firstly, new levels for control parameters are selected. Based on the level distribution diagram of the parameter in Fig. 2, we choose the new levels of control parameters as follows: The optimal parameters are levels with the largest value of the parameters, namely, k_{p1} level 3, k_{d1} level 3. Therefore, we have the values of the new levels as follows:

If level 1 is optimal then the next levels are

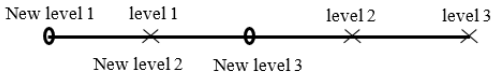

$$\begin{cases} \text{level 2\_new} = \text{level 1\_old} \\ \text{level 1\_new} = \text{level 1\_old} - \dfrac{\text{level 2\_old} - \text{level 1\_old}}{2} \\ \text{level 3\_new} = \text{level 1\_old} + \dfrac{\text{level 2\_old} - \text{level 1\_old}}{2} \end{cases}$$

If level 2 is optimal then the next levels are

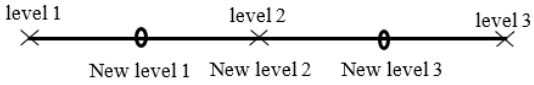

$$\begin{cases} \text{level 2\_new} = \text{level 2\_old} \\ \text{level 1\_new} = \text{level 2\_old} - \dfrac{\text{level 2\_old} - \text{level 1\_old}}{2} \\ \text{level 3\_new} = \text{level 2\_old} + \dfrac{\text{level 3\_old} - \text{level 2\_old}}{2} \end{cases}$$

If level 3 is optimal then the next levels are

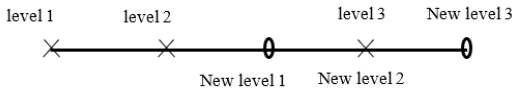

$$\begin{cases} \text{level 2\_new} = \text{level 3\_old} \\ \text{level 1\_new} = \text{level 3\_old} - \dfrac{\text{level 3\_old} - \text{level 2\_old}}{2} \\ \text{level 3\_new} = \text{level 3\_old} + \dfrac{\text{level 3\_old} - \text{level 2\_old}}{2} \end{cases}$$

According to the rule presented above, we have the new levels of control parameters in Table IV.

TABLE IV. CONTROL FACTORS AND NEW LEVELS OF CONTROL PARAMETERS

Levels	**Control parameters**	
	kp1	kd1
1	15	16.5
2	25	26
3	35	35

Then the analysis of signal-to-noise ratio is performed as the step 2.

Step 6: Check the convergence condition of the signal-to-noise ratio and determine the optimal control parameters

After 60 iterations, we obtain the optimal noise values of the control parameters with the results listed in Table V.

TABLE V. SNR VALUES OF THE CONTROL PARAMETERS AND ANOM AND ANOVA IN THE ROW OF THE SNR

Trial	Calculation Results			
	SNR (kp1)	SNR (kd1)	Mean	Variance
1	14.8697	8.4962	11.68295	10.15538
2	23.1742	20.9025	22.03835	1.290155
3	27.3572	28.9904	28.1738	0.666836
4	33.4549	34.104	33.77945	0.105333
5	44.2991	47.0856	45.69235	1.941146
…	…	…	…	…
56	274.9553	274.9553	274.9553	0
57	274.9553	274.9553	274.9553	0
58	274.9553	274.9553	274.9553	0
59	274.9553	274.9553	274.9553	0
60	274.9553	274.9553	274.9553	0

To determine the mean and variance of SNR we use the following formulas

$$\text{Mean} = \frac{\text{SNR}(k_{p1}) + \text{SNR}(k_{d1})}{2} \tag{51}$$

$$\text{Variance} = \frac{\left[\text{SNR}(k_{p1}) - \text{Mean}\right]^2 + \left[\text{SNR}(k_{d1}) - \text{Mean}\right]^2}{2} \tag{52}$$

According to the above analysis, we obtain the optimal parameters of after 60 iterations. The optimal control parameters are given as follows

$$k_{p1} = 37.1617,\ k_{d1} = 29.241 \tag{53}$$

Using these values, it is easy to find the optimal Floquet multipliers of Eq. (46).

$$\rho_1 = 0.3\ ,\ \rho_2 = 0, \rho_3 = 0,\ \rho_4 = 0. \tag{54}$$

C. Determine Control Parameters in a Number of Common Speed Ranges

We choose the desired motion rule of the active links such as Eq. (21)

$$q_a(t) = \pi/2 + \pi/2 \sin(\Omega t) \tag{55}$$

Using the algorithm presented in paragraph 3.2, we can determine the control parameters corresponding to some popular speed ranges as follows Table VI.

TABLE VI. CONTROL PARAMETERS IN SEVERAL SPEED RANGES

Ω	k_{p1}	k_{d1}	Ω	k_{p1}	k_{d1}
2π	37.1617	29.241	8π	23.0147	6.8628
4π	28.7617	11.7501	10π	20.1903	5.4368
6π	22.2666	6.7208	12π	15.0579	3.7541

IV. Approximate Calculation of Inverse Dynamics of Flexible Manipulator

In previous section, the stability analysis of the flexible manipulator has been studied. In this section an approximate method for calculation of inverse dynamics of flexible manipulator is proposed.

A. Calculating Periodic Oscillation of a Flexible Manipulator

The linearized differential equations of motion of the single-link flexible manipulator have the following form

$$\mathbf{M}_L^{(1)}(t)\ddot{\mathbf{y}} + \mathbf{C}_L^{(1)}(t)\dot{\mathbf{y}} + \mathbf{K}_L^{(1)}(t)\mathbf{y} = \mathbf{h}_L^{(1)}(t)\,. \tag{56}$$

As known in the theory of linear differential equations [24] when the system of homogeneous linear differential equations is asymptotically stable, then the system of differential equations having the right side Eq. (56) has periodic solution. Using the algorithm proposed by Khang *et al*. in [25], the periodic oscillation of the system of Eq. (56) can be calculated in the following form

$$\mathbf{y}^* = \left[\mathbf{y}_1^* \quad \mathbf{y}_2^*\right] \tag{57}$$

When the parameters $\mathbf{K}_P$ and $\mathbf{K}_D$ are chosen so that the system of homogeneous linear differential equations is asymptotically stable is stable quickly, the solution of Eq. (56) has the form

$$\mathbf{y} \approx \mathbf{y}^*\,. \tag{58}$$

Using the control parameters in Table VI, some simulation results of solutions of Eq. (51) are shown in Fig. 3.

From perturbed motions $\mathbf{y}$, we call determine the generalized coordinats, velocities and accelerations of flexible manipulator.

$$q_{ai}(t) \approx q_{ai}^R(t) + y_i(t),\ (i = 1,...,n);\ q_{ej}(t) = y_{n+j}(j = 1,...,m) \tag{59}$$

Case 1: $\Omega = 2\pi$

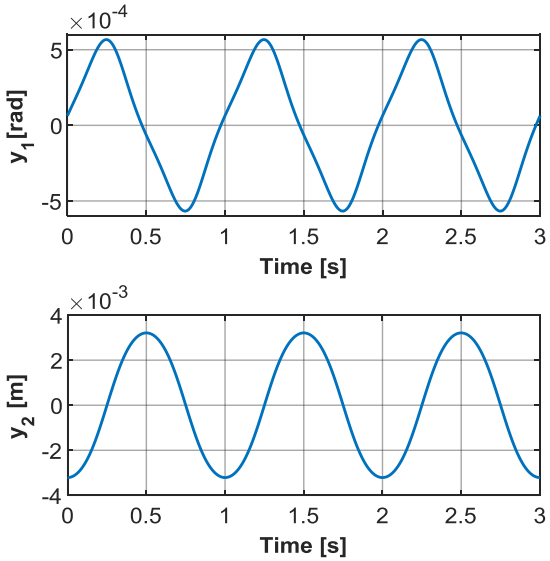

(a). Periodic vibrations of perturbed motions by $\Omega = 2\pi$.

Case 2: $\Omega = 6\pi$

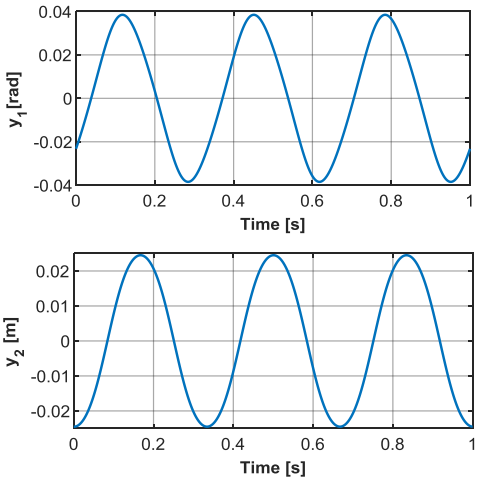

(b). Periodic vibrations of perturbed motions by $\Omega = 6\pi$

Case 3: $\Omega = 10\pi$

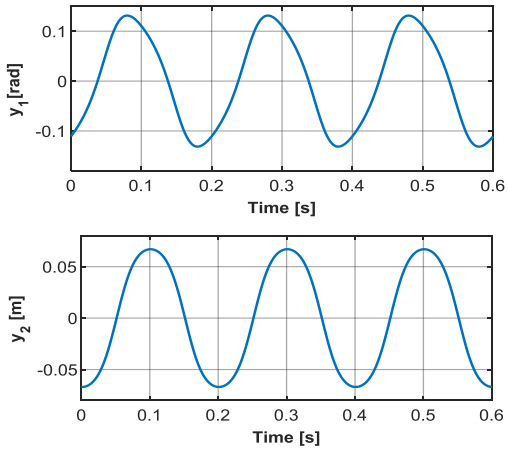

(c). Periodic vibrations of perturbed motions by $\Omega = 10\pi$

Figure 3. Periodic oscillation of perturbed motions.

B. Determining the Motion of the Operating Point E

From the periodic oscillation calculated above, we can find the elastic displacement of the elastic beam *OE* :

$$w(x,t) = X_1(x)y_2(t) \tag{60}$$

From Eq. (60) we have the elastic displacement from point E:

$$w(l,t) = X_1(l)y_2(t) \tag{61}$$

Then the position of the point E is given as:

$$x_E(t) = l\cos(q_a^R + y_1) - w(l,t)\sin(q_a^R + y_1) \tag{62}$$

$$y_E(t) = l\sin(q_a^R + y_1) + w(l,t)\cos(q_a^R + y_1) \tag{63}$$

From there the position error of the point E is determined by the following formula:

$$d_e = \sqrt{(x_E - x_E^R)^2 + (y_E - y_E^R)^2} \tag{64}$$

Using the control parameters in Table VI, some simulation results of the position of point E are shown in Fig. 4.

Case 1: $\Omega = 2\pi$

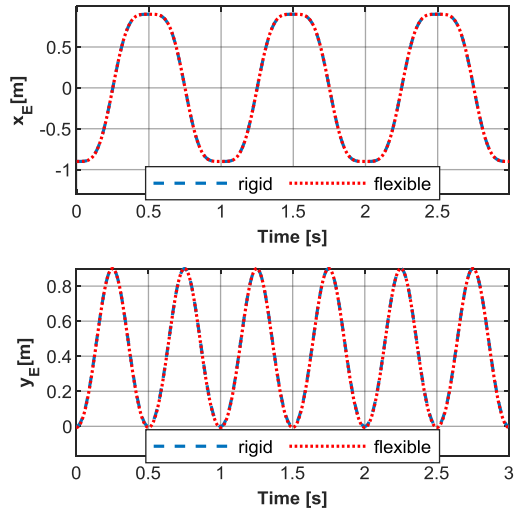

(a) Motion graph of operating point E by $\Omega = 2\pi$

Case 2: $\Omega = 6\pi$

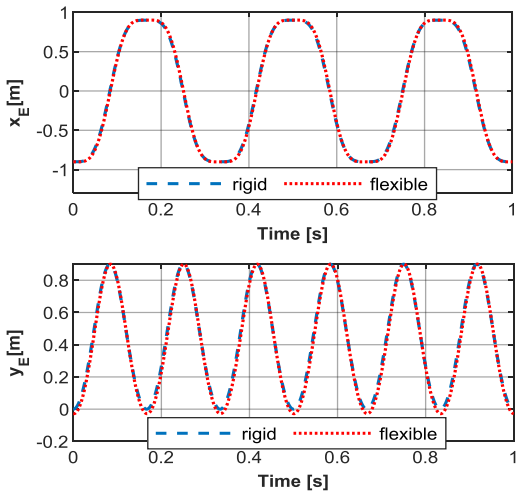

(b) Motion graph of operating point E by $\Omega = 6\pi$

Case 3: $\Omega = 10\pi$

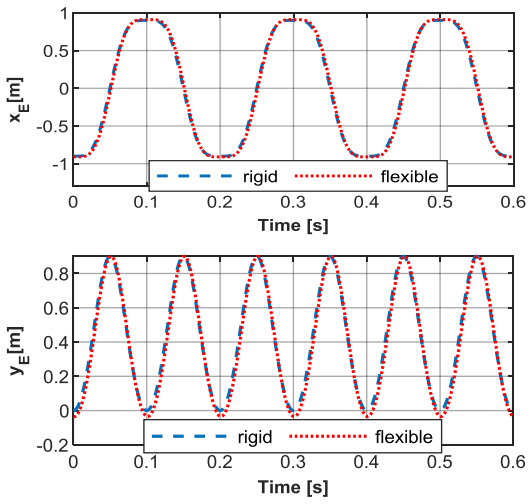

(c) Motion graph of operating point E by $\Omega = 10\pi$

Figure 4. Position of operating point E.

In Fig. 4, the dotted lines represent the motion graph of operation point E when the OE link is an elastic beam, the dashed lines represent the motion graph of operation point E when the OE link is a rigid link.

C. Calculating Inverse Dynamics of Flexible Manipulator

By substituting Eqs. (60)–(63) into Eq. (16) it get the actuator torque of a single-link flexible manipulator:

$$\begin{aligned}\tau &= M_d \\ &+\left[J_1 + m_E l^2 + \frac{1}{3}\rho A l^3 + (\rho A m_{11} q_e^2 + m_E X_1^2(l) q_e^2)\right]\ddot{q}_a \\ &+\left[\rho A D_1 + m_E l X_1(l)\right]\ddot{q}_e \\ &+\begin{bmatrix} 2m_E X_1^2(l) + 2\rho A m_{11}]\dot{q}_a \dot{q}_e q_e \\ +\dfrac{m_{OE} g l \cos q_a}{2} - \mu g \sin q_a C_1 q_e \\ +m_E g[l\cos q_a - X_1(l) q_e \sin q_a \end{bmatrix}\end{aligned} \tag{65}$$

The actuator torque of rigid system $\tau_a^R(t)$ is given as Eq. (22).

Using the control parameters in Table VI, some calculation results of actuator torque are shown in Fig. 5.

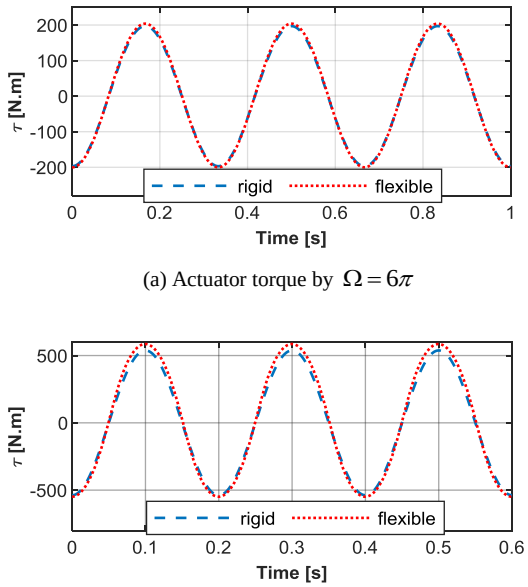

(a) Actuator torque by $\Omega = 6\pi$

(b) Actuator torque by $\Omega = 10\pi$

Figure 5. Simulation results of joint torques.

In Fig. 5, the dotted lines represent the joint torques when the OE link is an elastic beam, the dashed lines are the joint torques when the OE link is a rigid link. Through the graphs, we can see that when the angular velocity of the joint links is larger, the graph of the joint torques with elastic OE link is further away from the joint torque graph with solid link.

V. Conclusion

In the present paper, the linearization problem of the equation of motion of flexible manipulator in the vicinity of a fundamental motion is addressed. Then an approach

for the computation of dynamic stability control and the inverse dynamics of flexible manipulators has been presented.

A procedure for the optimal design of control parameters of the homogeneous linear differential equations having time-periodic coefficients is presented. In case the system is unstable, we need to design the controller for the motion of the flexible manipulator, a PD controller is added to stabilize the system. Then the optimal parameters of the PD controller are found by Taguchi method. The proposed approach has been successfully applied to a flexible manipulator. From the calculation of the oscillation of the flexible manipulator, substituting the coordinates into the motion equation of flexible manipulators, an algorithm for finding the actuator torques of the flexible manipulator has been implemented.

Through numerical simulation, the efficiency and usefulness of the proposed algorithm were demonstrated as well. It is believed that the results of this study can be extended to flexible multi-link manipulators, and thus, can be of great importance for slewing space structures where the transported object is sensitive to vibrations.

CONFLICT OF INTEREST

The authors declare no conflict of interest.

AUTHOR CONTRIBUTIONS

N.V.Q was originally responsible for conceptualization and methodology. B.T.H.L., D.Q.T., and N.T.T. verified the simulation data, data curation, investigation, and draft writing. N.H.Q. contributes a formal analysis of review, editing, and supervision. All authors have read and agreed to the published version of the manuscript.

ACKNOWLEDGMENT

The authors gratefully acknowledge Thai Nguyen University of Technology, Vietnam, for supporting this work.

REFERENCES

[1] E. Bayo, P. Papadopoulos, J. Stubbe, and M. A. Serna, "Inverse dynamics and kinematics of multi-link elastic robots: An iterative frequency domain approach," *The International Journal of Robotics Research*, vol. 8, no. 6, pp. 49-62, 1989.

[2] H. Asada, Z. D. Ma, and H. Tokumaru, "Inverse dynamics of flexible robot arms: Modeling and computation for trajectory control," *ASME Journal of Dynamic Systems, Measurement, and Control*, vol. 112, no. 2, pp. 177-185, 1990.

[3] B. C. Chiou and M. Shahinpoor, "Dynamic stability analysis of a two-link force-controlled flexible manipulator," *ASME Journal of Dynamic Systems, Measurement, and Control*, vol. 112, no. 4, pp. 661-666, 1990, doi: 10.1115/1.2896124.

[4] N. Poppelwell and D. Chang, "Influence of an offset payload on a flexible manipulator," *Journal of Sound and Vibration*, vol. 190, pp. 721-725, 1996, doi: 10.1006/jsvi.1996.0087.

[5] M. P. Coleman, "Vibration eigenfrequency analysis of a single-link flexible manipulator," *Journal of Sound and Vibration*, vol. 212, pp. 109-120, 1998, doi: 10.1006/jsvi.1997.1426.

[6] D. Li, J. W. Zu, and A. A. Goldenberg, "Dynamic modeling and mode analysis of flexible-link, flexible-joint robots," *Mechanism and Machine Theory*, vol. 33, pp. 1031-1044, 1998, doi: 10.1016/S0094-114X(97)00054-2.

[7] P. Kumar and B. Pratiher, "Modal characterization with nonlinear behaviors of a two-link flexible manipulator," *Archive of Applied Mechanics*, vol. 89, pp. 1201-1220, 2019, doi: 10.1007/s00419-018-1472-9.

[8] A. S. Yigit, "On the stability of PD control for a two-link rigid-flexible manipulator," *ASME Journal of Dynamic Systems, Measurement, and Control*, vol. 116, pp. 208-216, 1994, doi: 10.1115/1.2899212.

[9] S. Choura and A. S. Yigit, "Control of a two-link rigid–flexible manipulator with a moving payload mass," *Journal of Sound and Vibration*, vol. 243, pp. 883-897, 2001, doi: 10.1006/jsvi.2000.3449.

[10] A. A. Ata, W. F. Fares, and M. Y. Sa'adeh, "Dynamic analysis of a two-link flexible manipulator subject to different sets of conditions," *Procedia Engineering*, vol. 41, pp. 1253-1260, 2012, doi: 10.1016/j.proeng.2012.07.308

[11] W. Ding and Y. Shen, "Analysis of transient deformation response for flexible robotic manipulator using assumed mode method," in *Proc. 2017 2nd IEEE Asia-Pacific Conference on Intelligent Robot Systems (ACIRS)*, Wuhan, China, pp. 331-335, 2017, DOI: 10.1109/ACIRS.2017.7986118.

[12] X. Yang, S. S. Ge, and W. He, "Dynamic modeling and adaptive robust tracking control of a space robot with two-link flexible manipulators under unknown disturbances," *International Journal of Control*, vol. 91, pp. 969-988, 2018, doi: 10.1080/00207179.2017.1300837.

[13] Q. N. Hong, N. V. Quyen, and N. N. Hien, "Radial basis function neural network control for parallel spatial robot," *Telkomnika (Telecommunication Computing Electronics and Control)*, vol. 18, no. 6, pp. 3191-3201, 2020, DOI: 10.12928/telkomnika.v18i6.14913.

[14] C. C. Wit, B. Siciliano, and G. Bastin, eds., *Theory of Robot Control*, Springer Science & Business Media, Dec. 6, 2012.

[15] R. K. Roy, "A primer on the Taguchi method," *Society of Manufacturing Engineers*, 2010.

[16] G. Taguchi, S. Chowdhury, and Y. Wu, *Taguchi's Quality Engineering Handbook*, John Wiley & Sons, New Jersey, USA, 2005.

[17] R. A. Zambanini, "The application of Taguchi's method of parameter design to the design of mechanical systems," M.S. thesis, Lehigh University, Bethlehem, PA 18015 USA, 1992.

[18] N. V. Khang, D. T. Duong, N. T. V. Huong, N. D. T. T. Dinh, and V. D. Phuc, "Optimal control of vibration by multiple tuned liquid dampers using Taguchi method," *Journal of Mechanical Science and Technology*, vol. 33, pp. 1563-1572, 2019, DOI: 10.1007/s12206-019-0308-z.

[19] A. A. Shabana, "Flexible multibody dynamics: review of past and recent developments," *Multibody System Dynamics*, vol. 1, pp. 189-222, 1997, DOI: 10.1023/A:1009773505418.

[20] D. J. Inman, *Engineering Vibration (Second Edition)*, Prentice Hall, Englewood Cliffs, New Jersey, USA, 2001.

[21] J. N. Reddy, *Energy Principles and Variational Methods in Applied Mechanics*, John Wiley & Sons, New Jersey, USA, 2002.

[22] D. Jalon, J. G. and E. Bayo, *Kinematic and Dynamic Simulation of Multibody Systems: The Real-time Challenge*, Springer, 2012.

[23] P. D. Nguyen and M. C. Hoang, "Linearization and parametric vibration analysis of some applied problems in multibody systems," *Multibody System Dynamics*, vol. 22, pp. 163-180, 2009, DOI: 10.1007/s11044-009-9156-4.

[24] B. P. Demidovich, *Lectures on the Mathematical Stability Theory*, (in Rusian), Nauka, Moscow, 1967.

[25] V. N. Khang and N. P. Dien, "Parametric vibration analysis of transmission mechanisms using numerical methods," In: *Advances in Vibration Engineering and Structural Dynamics*, London, United Kingdom: IntechOpen, 2012, Ch. 12, pp. 301-331.